

Session VII

Linking the Halo with its Surroundings



Nobuo Arimoto building up Halos hierarchically.

Linking the Halo to its Surroundings

N. Arimoto

National Astronomical Observatory of Japan, Mitaka, Tokyo 181-8588, Japan

email: arimoto@optik.mtk.nao.ac.jp

Abstract. The Galactic halo is unlikely built up from galaxy populations similar to the dwarf spheroidal galaxies (dSph's) in the Local Group, but it is possible that the halo was formed by accreted dwarf galaxies that had much larger mass and higher star formation rates such as the Sagittarius dSph. Cosmological simulations show that dSph galaxies formed via hierarchical clustering of numerous smaller building blocks. Stars formed at the galaxy centre tend to form from metal-rich infall gas, which builds up the metallicity gradients. Infalling gas has larger rotational velocity and smaller velocity dispersion due to the dissipative processes, resulting the two distinct old stellar populations of different chemical and kinematic properties, which are recently discovered in the Sculptor dSph galaxy.

Keywords. Galaxy: abundances, Galaxy: halo, galaxies: abundances, galaxies: dwarf, galaxies: evolution, galaxies: formation, galaxies: halo, galaxies: stellar content, Local Group

1. Introduction

The origin of the Galactic dwarf spheroidal (dSph) galaxies is closely related to the formation and evolutionary history of the Milky Way. Modern cosmological models based on the Cold Dark Matter paradigm demonstrate the importance of hierarchical structure formation on all scales. Galaxies like the Milky Way and M31 form as part of a local overdensity in the primordial matter distribution via the agglomeration of numerous smaller building blocks that can independently develop into dwarf galaxies. In the Local Group the leftovers of this process are seen in the distribution and properties of the dwarf galaxies, with the dwarf spheroidals found mainly close in to the giant spirals, while the dwarf irregulars are more evenly distributed throughout the Local Group.

The gravitationally bound dwarf galaxies that have managed to avoid tidal destruction and subsequent merging have undergone episodic star formation over a Hubble time. The relatively gas-rich dwarf irregulars still exhibit ongoing star formation, while the dwarf spheroidals, being devoid of significant amounts of gas and dust, are now quiescent, and are therefore, in principle, much simpler systems to study. The proximity of the Galactic dSphs offers a unique opportunity for investigating galaxy formation and evolution in unprecedented detail by studying the photometric and spectroscopic properties of the dSph stellar populations.

In this respect, an important approach is to explore the chemical abundances in individual stars belonging to nearby dSph galaxies, and to compare them with abundances found in Galactic halo stars. Recently, various nearby dSph galaxies have been the subject of extensive studies concerning accurate abundance analyses based on high-dispersion spectroscopic observations using ground-based 8-m class telescopes (see Table 1).

Shetrone *et al.* (1998) analyzed the high-resolution spectra of four red giant stars in the Draco dSph galaxy observed with the KECK HIRES spectrograph. Smecker-Hane & McWilliam (1999) reported preliminary abundances in 14 stars in the Sagittarius dSph galaxy. Bonifacio *et al.* (2000) obtained high-resolution data of two giant stars in the Sgr

Table 1. Abundance analyses of dSph's stars with 8-10m telescopes

dSph	No. stars	Observatory	References
Sculptor	5	VLT/UVES	Shetrone <i>et al.</i> (2003)
	4	VLT/UVES	Geisler <i>et al.</i> (2005)
Ursa Minor	3	Keck/HIRES	Shetrone <i>et al.</i> (1998)
	3	Keck/HIRES	Shetrone <i>et al.</i> (2001)
	3	Subaru/HDS	Sadakane <i>et al.</i> (2004)
	8	Subaru/HDS	Sadakane <i>et al.</i> (2005)
Draco	4	Keck/HIRES	Shetrone <i>et al.</i> (1998)
	2	Keck/HIRES	Shetrone <i>et al.</i> (2001)
	1	Keck/HIRES	Fulbright <i>et al.</i> (2004)
Sextans	2	Keck/HIRES	Shetrone <i>et al.</i> (2001)
Sagittarius	2	VLT/UVES	Bonifacio <i>et al.</i> (2000)
	14	Keck/HIRES	Smecker-Hane & McWilliam (1999)
	10	VLT/UVES	Bonifacio & Caffau (2003) Bonifacio <i>et al.</i> (2004)
Carina	5	VLT/UVES	Shetrone <i>et al.</i> (2003)
Fornax	3	VLT/UVES	Shetrone <i>et al.</i> (2003)
Leo I	2	VLT/UVES	Shetrone <i>et al.</i> (2003)

dSph galaxy using the UVES spectrograph on the ESO 8.2m Kueyen telescope (VLT). Bonifacio *et al.* (2004) analyzed the high-resolution data of 10 giant stars in the Sgr dSph galaxy, and obtained abundances of O, Mg, Si, Ca, and Fe. They concluded that a substantial metal-rich population exists in Sgr dSph. High-dispersion data of a total of 13 giant stars in Draco, Ursa Minor, and Sextans dSph galaxies were analyzed by Shetrone *et al.* (2001). They found large internal dispersions in metallicity of all three galaxies. They also found that the relative abundances of α -elements, $[\alpha/Fe]$, are lower in dSph galaxies compared with those found in the halo field stars over the same range in metallicity, which hints a non-negligible contribution of Type Ia Supernovae (SNe Ia) during the early stage of chemical enrichment, but the number of stars observed was too small to make any conclusions. Shetrone *et al.* (2003) and Tolstoy *et al.* (2003) carried out extensive abundance analyses of 15 red giant stars in the Sculptor, Fornax, Carina, and Leo I dSph galaxies, and discussed the implications for understanding the history of galaxy formation. Shetrone *et al.* (2003) found that certain abundance patterns appear to be very similar between these four dSph galaxies and Ursa Minor, Draco, Sextans, and Sagittarius dSph galaxies examined in the literature; i.e., iron-peak elements, second *s*- and *r*-process elements all show Galactic halo-like patterns. The α -elements, however, can vary from galaxy to galaxy. Sculptor, Leo I, Sextans, Ursa Minor, and Sagittarius dSph galaxies show a slightly decreasing $[\alpha/Fe]$ pattern with increasing metallicity, while Fornax and Draco show roughly constant $[\alpha/Fe]$. No uniform picture for nucleosynthesis in dSph galaxies has yet appeared, and clearly more abundance data are desperately required.

2. Subaru/HDS Observation of Ursa Minor dSph

With the HDS (High Dispersion Spectrograph) on the Subaru Telescope, we obtained high-resolution optical region spectra of 11 RGBs in the Ursa Minor dSph galaxy (Sadakane *et al.* 2004; Sadakane *et al.* 2005). Observations were done in May 2001, May 2002, and

Table 2. Atmospheric parameters & $[Fe/H]$ of 11 Ursa Minor dSph Stars

Star	V	B-V	T_{eff}	$\log g$	V_t	$[Fe/H]$	S/N_{6200}
COS347	16.94	1.52	4050	0.3	2.1	-1.63	55
COS 4	16.73	1.33	4300	0.3	2.0	-2.66	50
COS 82	17.20	1.36	4300	0.3	2.0	-1.53	60
SCM1677	16.54	1.56	4050	0.0	3.0	-2.30	65
SCM 848	16.68	1.41	4150	0.1	1.9	-2.03	60
SCM1348	16.96	1.27	4350	0.5	1.8	-2.12	40
SCM 514	16.96	1.30	4250	0.5	2.0	-2.12	45
SCM 639	17.05	1.32	4300	0.5	2.0	-2.12	45
SCM 557	17.10	1.19	4350	0.8	1.9	-2.08	35
SCM1095	17.02	1.30	4450	0.9	2.0	-1.91	35
SCM1472	17.17	1.19	4300	0.5	2.0	-1.91	30

May 2004, with the wavelength coverage $4400\text{\AA} - 7160\text{\AA}$, slit width 1 arcsec, resolution $R = 39000$. Typical exposure time for each star was ~ 2 hours and the average S/N ratio (per pixel) ranged from 30 to 60. The chemical abundances in these stars were analyzed for 26 elements, including α -, iron-peak, and neutron-capture elements. Atmospheric parameters and resulting metallicities are given in Table 2. The metallicity spreads from $[Fe/H] = -2.66$ to -1.53 with an average $\langle [Fe/H] \rangle = -2.0 \pm 0.3$. As was already shown by Shetrone *et al.* (2001), $[Si/Fe]$, $[Ca/Fe]$, and $[Ti/Fe]$ are systematically lower than the Galactic counterparts, starting to decrease at around $[Fe/H] \simeq -2$ (Figure 1). The relative abundances of $[Si/Fe]$, $[Ca/Fe]$, and $[Ti/Fe]$ tend to lie below $[Mg/Fe]$. This may either suggest a lack of supernovae in the dwarf spheroidal galaxies (Venn *et al.* 2004) or may suggest an effective truncation of upper IMF with slow chemical enrichment (Tolstoy *et al.* 2003). $[Mn/Fe]$ shows a mirror images of $[\alpha/Fe]$, increasing at $[Fe/H] \simeq -2$. Low abundances of α -elements and high abundances of Mn seem to suggest a significant contribution of SNe Ia at low metallicity in the Ursa Minor dSph. Interestingly we find that Na is significantly depleted in most of the Ursa Minor stars. A similar Na deficiency was previously found for Sagittarius dSph galaxy, but at much higher metallicity ($[Fe/H] \geq -1.5$) (Bonifacio *et al.* 2000), may be due to the fact that Sagittarius dSph is more massive than the Ursa Minor dSph. Star formation rate (SFR) of dSph galaxies might depend on galaxy mass; i.e., higher SFRs for more massive dwarf galaxies, as has been suggested by an analysis of stellar density distribution on the colour-magnitude diagrams (Ikuta *et al.* 2005). This would imply that the onset metallicity of SNe Ia, $[Fe/H] \sim -2$ in the Ursa Minor dSph and $[Fe/H] \sim -1.5$ in the Sagittarius dSph, should become larger in more massive dSph galaxies due to higher SFRs. Then, one could conclude that the Galactic halo is unlikely built up from galaxy populations similar to the dSph's in the Local Group, but it is possible that the halo was formed by accreted dwarf galaxies that had much larger masses and hence higher SFRs.

In one star COS 82 ($[Fe/H] = -1.5$), however, we have found a large excess of heavy neutron-capture elements with a general abundance pattern similar to the scaled solar system *r*-process abundance curve. This is a bit puzzling, because it means there is no hint of an *s*-process (i.e., AGB stars) contribution, even at $[Fe/H] = -1.5$, suggesting that the SFR has been much stronger than that accounts for $[\alpha/Fe]$ increase at $[Fe/H] > -2$. One might be tempted to conclude that chemical enrichment in dSph galaxies had occurred in much smaller gaseous segments having wide variety of SFRs with inefficient mixing of materials that eventually fall on to the most massive clumps, finally becoming dSph galaxies one observes today.

3. Are Dwarf Galaxies Building Blocks?

Indeed, dwarf galaxies might not be the smallest unit (building blocks) of galaxy formation. We have imaged the smallest dwarf irregular galaxy in the Local Group, Leo A, by using Subaru/Suprime-Cam (Vanssevicius *et al.* 2004). Leo A is extremely gas rich and possesses very low stellar mass and metallicity. It contains young stars as well as old ones. It has been suggested in the past that Leo A has not experienced any strong event of merger or interaction for at least a few Gyrs; thus it is a good target for study of quiescent galaxy evolution.

In order to trace the entire extent of the old stellar populations in Leo A we employed the RGB stars. The following RGB star selection criteria have been applied: (1) location of stars in the color-magnitude diagram, I versus (V-I), within the zone marked in Figure 2; (2) high photometric accuracy, (3) good fit with the stellar point-spread function, and (4) photometric criterion devoted to wipe out the objects with nonstellar spectra, (B-V) – (V-I), in the range of -0.40 to $+0.10$. The ellipticity (ratio of semiminor to semimajor axis) deduced for the RGB star distribution $b/a = 0.60 \pm 0.03$ coincident with b/a of the H I envelope (Young & Lo 1996). For a detailed examination we selected the field located inside the ellipse ($b/a = 0.60$) of $a = 12'$ centered at the derived position, which is large enough to comfortably accommodate Leo A inside. We detected 1394 RGB stars distributed symmetrically and smoothly within this field.

Figure 3 shows the radial profile of the RGB star surface number density (arcmin^{-2}) of Leo A which was constructed by integrating within elliptical ($b/a = 0.60$) rings of width. Five distinct radial profile zones are noticeable: (1) a crowded central part, $a = 0.0' - 2.0'$ (2) an old exponential disc extending far beyond the previously estimated size of the galaxy (Mateo 1998), $a = 2.0' - 5.5'$; (3) the discovered stellar component in Leo A, which we call “halo,” $a = 5.5' - 7.5'$; (4) a sharp cutoff of the RGB star distribution

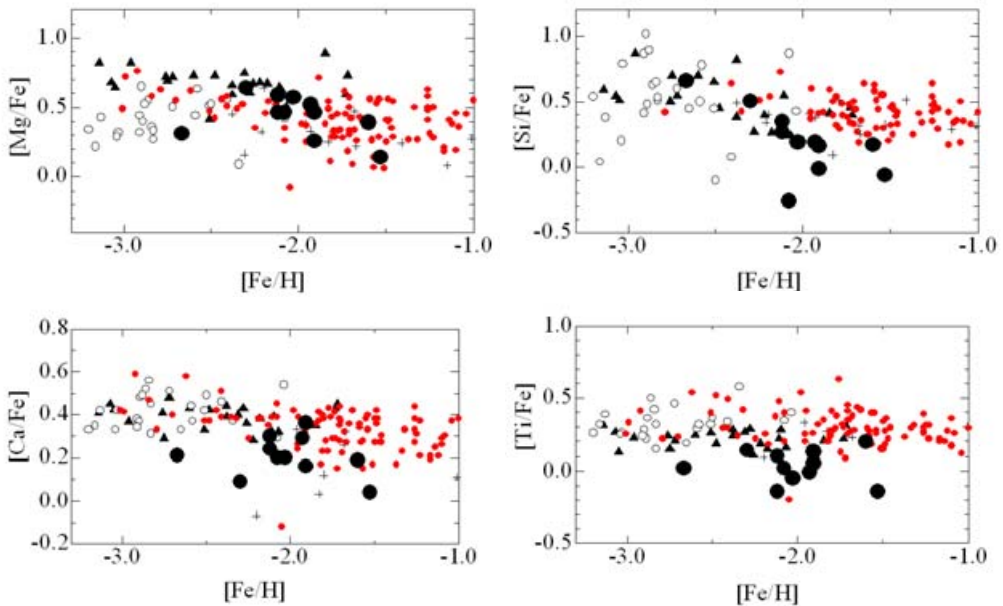


Figure 1. $[\alpha/\text{Fe}]$ vs $[\text{Fe}/\text{H}]$ relations for eleven Ursa Minor stars (large filled circles) and for Galactic metal-poor stars (small symbols) taken from Gratton & Sneden (1987), McWilliam *et al.* (1995), Fulbright (2000), and Johnson (2002).

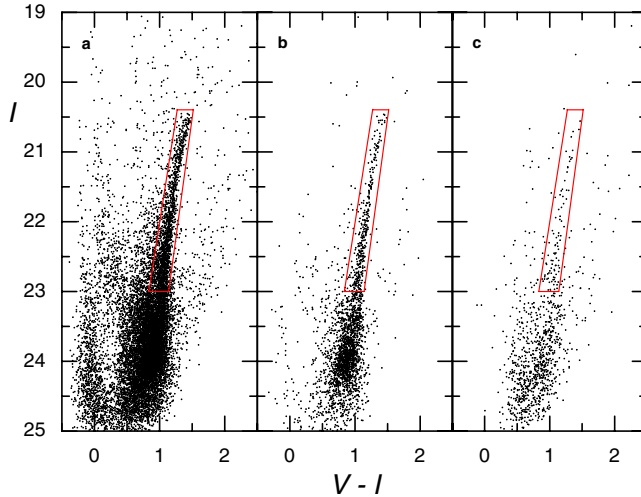


Figure 2. Colour-magnitude diagrams of the stellar-like objects in Leo A. The objects are shown (a) in the elliptical ($b/a = 0.6$) area, $a < 12'$, containing Leo A and its surroundings, the number of objects plotted, $N = 12,604$; (b) in the representative old disc area, $3' < a < 5'$, $N = 2,462$; (c) in the discovered halo area, $5.5' < a < 7.5'$, $N = 974$. The RGB stars employed for the structure analysis of Leo A were selected from the zone marked by lines.

coincident with the observed edge (Young & Lo 1996) and predicted cutoff of the H I envelope (Sternberg *et al.* 2002), $a = 7.5' - 8.0'$; and (5) a sky background zone where we derived a number density of contaminants to the RGB stars, $a = 8.0' - 12.0'$.

From the determined radial profile of the RGB stars, it is straightforward to evaluate the stellar mass of the old stellar population in Leo A. Assuming a Salpeter initial mass function and a stellar mass range of 0.5 to $100M_{\odot}$, we derived the mass of $\sim (4 \pm 2) \times 10^6 M_{\odot}$. This is in agreement with a recent estimate of the total stellar mass, $2.3 \times 10^6 M_{\odot}$, in Leo A (Lee *et al.* 2003) and confirms the very low mass of the galaxy's stellar populations.

We performed a halo-disc radial profile decomposition considering two extreme cases: (1) when the exponential disc, scale length 1.703 , is subtracted as the primary population, the remaining halo mass is $\sim 3\%$ of the disc mass; and (2) when the exponential halo, scale length 1.784 , is assumed to be a primary population, the halo mass is $\sim 30\%$ of the disc mass. The estimated lower and upper mass fractions of the halo are comparable to the Milky Way's halo and thick disc cases (Robin *et al.* 2003), respectively.

We conclude that the young and old Leo A discs, together with the discovered old halo and sharp stellar edge, closely resemble basic structures found in the large well grown-up disc galaxies. In the Cold Dark Matter cosmology scenarios, galaxies are assumed to build up and develop their internal structure via hierarchical merging of the primordial density fluctuations into larger systems. Therefore, our discovery of the stellar populations possessing distinct spatial distributions in the undisturbed very low mass Leo A suggests that even such a small system can be built via merging of much smaller segments; in other words, dwarf galaxies, both spheroidals and irregulars, are not the building blocks, but instead they themselves formed from much smaller building blocks.

Another evidence for complex early evolution of dSph galaxies is recently discovered by Tolstoy *et al.* (2004) who found evidence for the presence of two distinct ancient

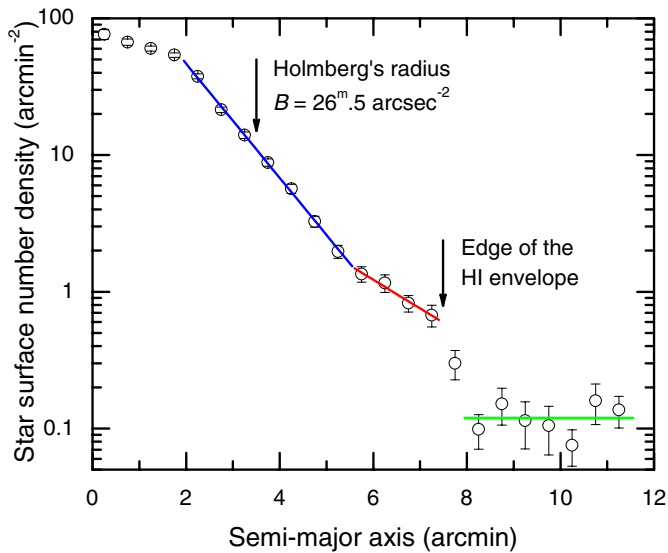


Figure 3. Radial profile of the RGB star surface number density in Leo A.

stellar components (both ≥ 10 Gyr old) in the Sculptor dSph by using the ESO Wide Field Imager in conjunction with the VLT/FLAMES spectrograph. They find that two components are discernible in the spatial distribution of HB stars in their imaging and in the $[Fe/H]$ and v_{hel} distributions for their large sample of spectroscopic measurements. The Sculptor dSph is composed of a “metal-poor” component ($[Fe/H] < -1.7$) and a “metal-rich” component ($[Fe/H] > -1.7$). The metal-poor stars are more spatially extended than the metal-rich ones, and they also appear to be kinematically distinct; i.e., the higher metallicity stars show velocity dispersion lower than that of lower metallicity stars. Therefore, both the Leo A dIrr and the Sculptor dSph galaxies indicate that even these simplest of galaxies appear to have had a surprisingly complex early evolution, and chemical enrichment as well.

4. Dwarf Spheroidal Formation as First Galaxy Formation

Paying particular attention to the most recent observational results of the Sculptor dSph in Tolstoy *et al.* (2004), we study the formation scenario of the dwarf spheroidal observed in the Local Group. Here, we test a scenario that the dSph is a small system which formed at a high redshift as a first generation of galaxies, and survived from cannibalization by a larger galaxy. We study the chemical and kinematic properties of the first galaxies which form at a high redshift, using high resolution cosmological numerical simulations, and compared them with the recent observational results of the Sculptor dSph. We demonstrate that the first galaxy can explain the observational trend as a result of the metallicity gradient induced by dissipative collapse of the gas component. Here we present an example of our series of evolutionary models, while the details of the models will appear elsewhere (Kawata *et al.* 2005).

The simulation was carried out using the galactic chemodynamics code, GCD+ (Kawata & Gibson 2003). GCD+ is a three-dimensional tree N -body/smoothed particle

hydrodynamics (SPH) code which incorporates self-gravity, hydrodynamics, radiative cooling, star formation, supernovae (SNe) feedback, and metal enrichment. GCD+ takes account of the chemical enrichment by both Type II (SNe II) and Type Ia (SNe Ia) SNe, mass-loss from intermediate mass stars, and follows the chemical enrichment history of both the stellar and gas components of the system.

We adopt a Λ CDM cosmology of $\Omega_0 h^2 = 0.135$, $\Lambda_0 = 1 - \Omega_0$, $\Omega_b h^2 = 0.0224$ and $h = 0.71$, and use a multi-resolution technique to achieve high-resolution in the regions of interest, including the tidal forces from neighboring large-scale structures. Gas dynamics and star formation are included only within the relevant high-resolution region (~ 80 kpc in comoving scale); the surrounding low-resolution region (~ 530 kpc diameter sphere) contributes to the high-resolution region only through gravity.

The first galaxies are expected to form at a higher density region, i.e., a biased region. Thus, we adopt a higher value of $\sigma_8 = 1.8$ to mimic the biased region. In the high-resolution region, we found a small stellar system at $z = 5.9$. The virial radius and mass of this system are respectively 3.2 kpc and $6.8 \times 10^7 M_\odot$ at $z = 5.9$. We assume that at this redshift star formation in this system has been quenched by some mechanisms, such as re-ionization and/or galactic wind, and the system evolves passively afterwards. Thus, we assume that the chemical and kinematic properties at $z = 5.9$ would not change till $z = 0$, and analyze the properties expected at $z = 0$ from the output of the simulation at $z = 5.9$.

The system is formed via hierarchical clustering of smaller building blocks involving some minor mergers, but global picture is somewhat similar to a monolithic collapse. Our assumed SNe feedback (7.5×10^{50} erg per supernova which is chosen to reproduce the low metallicity of the Sculptor dSph) has strong effect on the gas dynamics, and continuously blows out the gas from the system. However, the continuous gas accretion still leads to continuous star formation. Nevertheless, star formation of this small system is strongly suppressed by SNe feedback, which helps to keep the stellar metallicity low.

The metallicity distribution function for the inner $R < 0.25$ kpc (outer $R > 0.25$ kpc) region of the simulated galaxy has a peak at $[\text{Fe}/\text{H}] \sim -1.4$ ($[\text{Fe}/\text{H}] \sim -1.9$), which is consistent with the observed metallicity distribution functions in Tolstoy *et al.* (2004). Therefore, the simulated galaxy also show two distinct stellar populations. This is because, although dSph galaxies formed via hierarchical clustering, stars formed from cold dissipative gas in a similar fashion to a monolithic collapse scenario.

The observed velocity dispersions show that σ of the high metallicity ($[\text{Fe}/\text{H}] > -1.7$) stars is lower than that of the low metallicity ($[\text{Fe}/\text{H}] < -1.7$) stars. Our simulation results also show the same trend; i.e., the velocity dispersion decreases towards larger radius and σ of metal-poor stars is systematically larger than that of metal-rich ones at all radius, although the difference is small. Hence, our simulation demonstrates that a system formed at a high redshift can reproduce the two stellar populations whose chemical and dynamical properties are distinctive.

However, the simulated galaxy shows some inconsistent results with the observed properties of the Sculptor dSph. First, compared with Figure 3 of Tolstoy *et al.* (2004), the metallicity distribution functions for both the inner and outer regions of the simulated galaxy have a too long tail at lower $[\text{Fe}/\text{H}]$. In the observational data, there is no stars at $[\text{Fe}/\text{H}] < -2.8$. (Tolstoy *et al.* (2004) selected their samples from the limited region of the color-magnitude diagram, which might tend to exclude too low and too high metallicity stars). On the other hand, the simulated galaxy has a significant fraction of stars with such low metallicity. This is the so-called notorious ‘‘G-dwarf problem’’ which was originally found for the solar neighbourhood disc stars by van den Bergh (1962) and re-discovered for elliptical galaxies by Greggio (1997). Compared to the solar

neighbourhood disc, the metallicity range shifts towards much lower levels, but overproduction of low metal stars is a fatal problem of modeling the dSph galaxies. The solutions suggested for the solar neighbourhood “G-dwarf problem” include 1) gas infall, 2) prompt initial enrichment (PIE), and 3) metal-enhanced star formation (MESF). The infall model has been so far very successful in solving the local G-dwarf problem, as it is likely that the disc of Milky Way has been formed by continuous accretion of gas from the reservoirs (Galactic halo and/or extragalactic dwarf galaxies). However, it is rather unlikely in the case of our model simulation of dSph galaxies, since such a cosmological infall is already taken into account as a basic physics of galaxy formation. The MESF model is unlikely either, as it is also fully taken into account in the modeling by introducing different cooling efficiency for the gas of different metallicity. This leaves the PIE scenario as the only possibility for solving the “G-dwarf problem” of the dSph galaxies. The chemical enrichment should have occurred in individual gas clumps even before they accreted onto the main body of the dSph galaxy and local enrichment due to nearby supernovae and local mixing of interstellar turbulence may result in different efficiency of the enrichment (as we have seen for the case of COS82 in the Ursa Minor dSph), but the chemical enrichment process as a whole should be very similar to the classical “simple model” of galactic chemical evolution. Thus, stars should have formed from metal-free gas at the beginning. Only if most of small gaseous clumps had already been contaminated by preceding supernovae or whatever else the “G-dwarf problem” of the dSph galaxies would disappear. This might suggest a possible Population III event of very low enrichment level prior to the formation of low mass galactic clumps.

As we have shown in our Subaru/HDS observation of the Ursa Minor dSph, the stars in dSph galaxies show different distributions in the $[\alpha/Fe]$ vs $[Fe/H]$ plane, compared with the stars in the solar neighborhood. In the Sculptor dSph, $[\alpha/Fe]$ of the member stars with $[Fe/H] < -2$ are higher than the solar abundance ratios, and $[\alpha/Fe]$ approach the solar value as $[Fe/H]$ increases at $[Fe/H] > -2$ (Tolstoy (2005) and Kim Venn’s talk at this conference). On the other hand, in the solar neighborhood $[\alpha/Fe]$ are constantly higher than the solar value for the stars with $[Fe/H] < -1$, and start decreasing at $[Fe/H] = -1$. This difference can be explained by the contribution from SNe Ia, which decrease $[\alpha/Fe]$, and a lower SFR in the dSph, which keeps $[Fe/H]$ low till the chemical enrichment by SNe Ia becomes important (Ikuta & Arimoto (2002)). However, in our model, we find that the mean $[O/Fe]$ is almost constant (oxygen is one of typical α -element). This is because we implemented an SNe Ia model proposed by Kobayashi *et al.* (2000) who suggested that SNe Ia are inhibited in the stars with $[Fe/H] < -1$. The simulated galaxy has the SFR small enough to keep $[Fe/H]$ low, and the duration of star formation is longer than the life-time of the expected SNe Ia progenitors. Hence, if we did not assume the suppression of SNe Ia at the low $[Fe/H]$, we expect that our simulation can explain the observational trend.

Finally we should note that the velocity dispersion of our simulated galaxy ($\sigma \simeq 7$ km sec⁻¹) is too small compared with the observed values ($\sigma \simeq 10$ km sec⁻¹). In addition, the total V-band magnitude of the simulated galaxy ($M_V = -7.23$), which is also small, compared with the luminosity of the Sculptor dSph ($M_V = -10.7$). We have tried the different parameter sets of models for star formation and SNe feedback. However, we found that to keep metallicity as low as what is observed, the strong SNe feedback which leads to the low efficiency of star formation is required, which makes it difficult to produce enough stars at a high redshift. The simplest solution is that tens of such small systems made “dry” merger without any additional star formation. However, it is unlikely, and such mergers would smear out a metallicity gradient completely. Alternatively, they might have been more massive in the past and were able to continue a low level of star

formation even after the re-ionization in the inner region (see Kawata *et al.* (2005) for more detailed arguments). We hope that our present study would be a good starting point to test the formation scenario of the dSph galaxies, comparing the detailed observation with chemo-dynamical galaxy formation models.

5. Conclusions

We have conducted Subaru/HDS observation of 11 RGB stars in the Ursa Minor dSph galaxy. By comparing the abundance patterns of α -elements, Mn, Na, *s*- and *r*-process elements of Ursa Minor stars to those of Galactic halo stars of equivalent metallicity, we conclude that the Galactic halo is unlikely built up from galaxy populations similar to the dSph's in the Local Group, but it is possible that the halo was formed by accreted dwarf galaxies that had much larger mass and hence higher SFRs.

We have discovered the stellar populations having distinct spatial distribution in the undisturbed very low mass Leo A dwarf irregular galaxy with Subaru/Suprime-Cam. We conclude that the young and old discs, together with the discovered old halo and sharp stellar edge, closely resemble basic structures found in the large full-fledged disc galaxies. This suggests complex formation histories even in very low mass galaxies such as Leo A and challenges contemporary understandings of galaxy evolution. Dwarf galaxies are likely grown-up via the agglomeration of numerous smaller building blocks.

We have analyzed chemical and kinematic properties of a small system which formed at a high redshift in the Λ CDM cosmology. In this simulation, dSph galaxies formed hierarchically but with no significant major mergers and the galaxy formation history looks very similar to a monolithic collapse formation (ie., continuous accretion of gas clumps with occasional minor mergers). Our simulated galaxy shows that the higher metallicity ($[Fe/H] > -1.7$) stars have more centrally concentrated distribution and lower velocity dispersion, compared with the lower metallicity stars ($[Fe/H] < -1.7$). This trend is consistent with the observed trend in the Sculptor dSph. Thus, we conclude that a survivor of a small system which formed at a high redshift can explain the observed stellar chemical and kinematic properties of dwarf spheroidal galaxies.

Acknowledgements

This work was financially supported in part by a Grant-in-Aid for the Scientific Research (No.16540223) by the Japanese Ministry of Education, Culture, Sports and Science.

References

- Bonifacio, P., Sbordone, L., Marconi, G., Pasquini, L., & Hill, V. 2004, *A&A* 414, 503
 Bonifacio, P. & Caffau, E. 2003, *A&A* 399, 1183
 Bonifacio, P., Hill, V., Molaro, P., Pasquini, L., Di Marcantonio, P., & Santin, P. 2000, *A&A* 359, 663
 Geisler, D., Smith, V. V., Wallerstein, G., Gonzalez, G., & Charbonnel, C. 2005, *AJ* 129, 1428
 Gratton, R.G. & Sneden, C 1987, *A&A* 178, 179
 Greggio, L. 1997, *MNRAS* 285, 151
 Fulbright, J.P., Rich, R.M. & Castro, S. 2004, *ApJ* 612, 447
 Fulbright, J.P. 2000, *AJ* 120, 1841
 Ikuta, C., Arimoto, N., & Jablonka, P. 2005, *in preparation*
 Ikuta, C. & Arimoto, N. 2002, *A&A* 391, 55
 Johnson, J.A. 2002, *ApJS* 139, 219
 Kawata, D., Arimoto, N., Cen, R., & Gibson, B. 2005, *submitted to ApJ*

- Kawata, D. & Gibson, B.K. 2003, *MNRAS* 346, 135
- Kobayashi, C., Tsujimoto, T., & Nomoto, K. 2000, *ApJ* 539, 26
- Lee, H., McCal, M.L., & Richer, M.G. 2003, *AJ* 125, 2975
- Mateo, M. 1998, *ARA&A* 36, 435
- McWilliam, A., Preston, G.W., Sneden, C., & Searle, L. 1995, *AJ* 109, 2757
- Robin, A.C., Reylé, C., Derrière, S., & Picaud, S. 2003, *A&A* 409, 523
- Sadakane, K., Arimoto, N., Aoki, W., Ohkubo, M., Ohnishi, K., & Tajitsu, A. 2005,
- Sadakane, K., Arimoto, N., Ikuta, C., Aoki, W., Jablonka, P., & Tajitsu, A. 2004, *PASJ* 56, 1041
- Shetrone, M., Venn, K.A., Tolstoy, E., Primas, F., Hill, V., & Kaufer, A. 2003, *AJ* 125, 684
- Shetrone, M.D., Côté, P., & Sargent, W.L.W. 2001, *ApJ* 548, 592
- Shetrone, M.D., Bolte, M., & Stetson, P.B. 1998 *AJ* 115, 1888
- Smecker-Hane, T.A. & McWilliam, A. 1999, *ASPC* 192, 150
- Sternberg, A., McKee, Ch, & Wolfire, M.G. 2002, *ApJS* 143, 419
- Tolstoy, E. 2005, *astro-ph*, 0506481
- Tolstoy, E., *et al.* 2004, *ApJL* 617, L119
- Tolstoy, E., Venn, K., Shetrone, M., Primas, F., Hill, V., Kaufer, A., & Szeifert, T. 2003, *AJ* 125, 707
- Vansevicius, V., Arimoto, N., Hasegawa, T. *et al.* 2004, *ApJL* 611, L93
- van den Bergh, S. 1962 *AJ* 67, 486
- Venn, Kim A., Irwin, Mike, Shetrone, Matthew D., Tout, Christopher A., Hill, Vanessa, & Tolstoy, Eline 2004, *AJ* 128, 1177
- Young, L.M. & Lo, K.Y. 1996, *ApJ* 462, 203